doi: 10.15407/ujpe62.10.0835

B.E. GRINYUK, D.V. PIATNYTSKYI
Bogolyubov Institute for Theoretical Physics, Nat. Acad. of Sci. of Ukraine
(14b, Metrolohichna Str., Kyiv 03680, Ukraine; e-mail: bgrinyuk@bitp.kiev.ua)

PACS 27.20.+n, 1.60.Gx, 21.10.Ft, 21.10.Gv

STRUCTURE OF ^{14}N NUCLEUS WITHIN A FIVE-CLUSTER MODEL

The spatial structure of ^{14}N nucleus is studied within a five-particle model (three α-particles plus two nucleons). Using the variational approach with Gaussian bases, the ground-state energy and wave function are calculated for this five-particle system. Two spatial configurations in the ground-state wave function are revealed. The density distributions, pair correlation functions, and the momentum distributions of particles are analyzed and compared with those of the mirror nuclei ^{14}C and ^{14}O.

Keywords: cluster structure of ^{14}N nucleus, charge density distribution, pair correlation functions, momentum distributions.

1. Introduction

In the present paper, we study the structure characteristics of ^{14}N nucleus as a system of three α-particles and two extra nucleons (a neutron and a proton). A steady interest in the structure of this nucleus can be explained, in particular, by its important role in the nuclear fusion reactions in stars.

Our five-particle approach may have a rather good accuracy, as it was shown by calculations of the structure functions of three- and four-cluster nuclei [1–5] consisting of α-particles and two extra nucleons. The similar five-particle model [6] was considered to predict the charge radius of ^{14}O nucleus using the closeness of the structures of mirror nuclei ^{14}C and ^{14}O.

The α-particle clusters are known to be too tightly bound systems of four nucleons (with 28.3 MeV binding energy of ^{4}He nucleus) and to have a too small polarizability, so that they can be considered as structureless particles, as long as one can ignore their excitation at the impact energy greater than $\sim$20 MeV. Although the initial Hamiltonian contains "pointlike" α-particles, we will consider, after the first-stage calculations, their size and their own density distributions in the Helm approximation (see below). In principle, the nucleon structure of α-particles could be taken into account more accurately [1], if one multiplies the wave function of the nucleus obtained within the α-particle model by the wave functions of the ^{4}He nuclei obtained independently in terms of their nucleon degrees of freedom, and then antisymmetrizes the total wave function with respect to identical nucleons. For the ground state of a nucleus and some low-lying energy levels (for which the excitation of an α-particle can be neglected), our five-particle model can be competitive in accuracy with the approaches like [7], where one has to deal with all the nucleon degrees of freedom and thus to resolve a more complicated problem.

For the five-particle problem, we exploit the variational method with Gaussian bases [8, 9] widely used to study the bound states of few-particle systems.

In the next section, the interaction potentials between particles are given. In Section 3, we discuss the r.m.s. radii and density distributions of particles in ^{14}N nucleus. Relative distances between particles and pair correlation functions are presented in Section 4. Section 5 dwells upon two spatial configurations in the ground state of ^{14}N. In Section 6, the momentum distributions are given. Almost in all the cases, we compare the corresponding structure functions of ^{14}N nucleus with those of ^{14}C and ^{14}O within the same five-particle model.

2. Statement of the Problem

Within our model, the five-particle Hamiltonian for ^{14}N

$$\hat{H} = \frac{\mathbf{p}_1^2}{2m_p} + \frac{\mathbf{p}_2^2}{2m_n} + \sum_{i=3}^{5} \frac{\mathbf{p}_i^2}{2m_\alpha} + \\ + U_{pn}\left(r_{12}\right) + \sum_{j>i=3}^{5} \hat{U}_{\alpha\alpha}\left(r_{ij}\right) + \\ + \sum_{j=3}^{5} \hat{U}_{p\alpha}\left(r_{1j}\right) + \sum_{j=3}^{5} \hat{U}_{n\alpha}\left(r_{2j}\right) + \sum_{j>i=1}^{5} \frac{Z_i Z_j e^2}{r_{ij}} \qquad (1)$$

contains, in addition to the kinetic energy, pairwise potentials due to nuclear and Coulomb interactions between particles. In expression (1), the indices p, n, and α denote a proton, neutron, and α-particle, respectively. In the Coulomb term, Z_i are the charges of particles in units of elementary charge e: $Z_1 = 1$ for an extra proton, $Z_2 = 0$ for an extra neutron, and $Z_3 = Z_4 = Z_5 = 2$ for α-particles. The nuclear potential $U_{pn}(r_{12})$ between the extra nucleons in the triplet state is used in the form of a local potential proposed in [10] with two Gaussian terms describing the attraction (with intensity -146.046 MeV and radius 1.271 fm) and the repulsion (with intensity 840.545 MeV and radius 0.44 fm). This simple potential gives correct experimental values for the deuteron binding energy $\varepsilon_{\mathrm{d}} = 2.224576$ MeV and charge radius $R_{\mathrm{d}} = 2.140$ fm, as well as experimental triplet np-scattering length $a_{np,t} = 5.424$ fm, and a good description of the np phase shift in the triplet state (up to $\sim$300 MeV). This potential was successfully used [10–12] for studying the ^{6}Li nucleus structure functions and their asymptotics.

The potentials $U_{n\alpha}$ and $U_{p\alpha}$, as well as the interaction potential between α-particles $U_{\alpha\alpha}$, are of a generalized type with local and nonlocal (separable) terms. This type of potentials was first proposed in [13, 14] to simulate the exchange effects between particles in interacting clusters and was successfully used, in particular, in calculations [1, 3, 5, 6] of multicluster nuclei. Parameters of the potentials $\hat{U}_{p\alpha}$ and $\hat{U}_{n\alpha}$, having local attraction and separable repulsion, are given in [6], where these potentials were used to study the structure of mirror nuclei ^{14}C and ^{14}O. As for the potential $\hat{U}_{\alpha\alpha}$ between α-particles, its parameters slightly differ from those used in [6]. This little change was necessary to reproduce accurately the experimental energy and charge radius of ^{14}N nucleus. In the local part of the interaction potential consisting of two Gaussian terms, we use the same intensity of a local attraction -43.5 MeV and that of a local repulsion 240.0 MeV, but with a little bit enlarged radii: 2.746 fm and 1.530 fm, respectively. The separable repulsion of the $\hat{U}_{\alpha\alpha}$ potential [6] is not changed.

The ground-state energy and the wave function are calculated with the use of the variational method in the Gaussian representation [8, 9], which proved its high accuracy in calculations of few-particle systems. For the ground state of the five-particle system (consisting of three α-particles plus two additional nucleons), the wave function can be expressed in the form

$$\Phi = \hat{S} \sum_{k=1}^{K} C_k \varphi_k \equiv \\ \equiv \hat{S} \sum_{k=1}^{K} C_k \exp\left(- \sum_{j>i=1}^{5} a_{k,ij} \left(\mathbf{r}_i - \mathbf{r}_j\right)^2 \right), \qquad (2)$$

where $\hat{S}$ is the symmetrization operator with respect to the coordinates of identical α-particles, and the linear coefficients C_k and nonlinear parameters $a_{k,ij}$ are variational parameters. The greater the dimension K of the basis, the more accurate the result is obtained. Note that, at any K, the trial wave function is exactly invariant with respect to translations in space, and, thus, the calculated center of mass kinetic energy is known to be exactly zero. The linear coefficients C_k can be found within the Galerkin method from the system of linear equations determining the energy of the system:

$$\sum_{m=1}^{K} C_m \left\langle \hat{S}\varphi_k \left| \hat{H} - E \right| \hat{S}\varphi_m \right\rangle = 0, \quad k = 0, 1, ..., K. \qquad (3)$$

The matrix elements in (3) are known to have explicit form for potentials like the Coulomb potential or the ones admitting a Gaussian expansion. Our potentials between particles just have the form of a few Gaussian functions, including the Gaussian form factor in the separable repulsive term. Thus, system (3) becomes a system of algebraic equations. We achieved the necessary high accuracy by using up to $K = 600$ functions of the Gaussian basis. To fix the nonlinear variational parameters $a_{k,ij}$, we used both the stochastic approach [8, 9] and regular variational methods. This enables us to obtain the best accuracy at reasonable values of the dimension K. Note that we solved, in fact, the five-particle problem a number of times, by fitting the parameters of the potentials in order to obtain the experimental binding energy of ^{14}N nucleus (19.772 MeV subtracting the own binding energy of α-particles) and its charge radius (2.558 fm [15]).

As a result of calculations, we have the ground-state wave function of ^{14}N nucleus within the five-particle model. This enables us to analyze the structure functions of this nucleus. In the next section, the density distributions of particles and the charge density distribution in ^{14}N are discussed.

3. Density Distributions and R.M.S. Radii of ^{14}N Nucleus

The probability density distribution $n_i(r)$ of the i-th particle in a system of particles with the wave function $|\Phi\rangle$ is known to be

$$n_i(r) = \langle\Phi|\,\delta\left(\mathbf{r} - (\mathbf{r}_i - \mathbf{R}_{\text{c.m.}})\right)|\Phi\rangle, \tag{4}$$

where $\mathbf{R}_{\text{c.m.}}$ gives the location of the center of mass of the system. The probability density distributions are normalized as $\int n_i(r)\,d\mathbf{r} = 1$.

In Fig. 1, we depict the values $r^2 n_p(r)$, $r^2 n_n(r)$, and $r^2 n_\alpha(r)$, respectively, for the density distributions (multiplied by r^2) of an extra proton, extra neutron, and α-particles in ^{14}N nucleus. Note that similar profiles were obtained for ^{14}C and ^{14}O nuclei in [6], and this means that ^{14}N nucleus may have almost the same structure. It is clearly seen that the extra nucleons in such a five-particle nuclei move mainly inside ^{12}C cluster formed by α-particles. The small secondary maximum of curve *1* at $r \approx 3.4$ fm shows that an extra proton (as well as an extra neutron) in ^{14}N nucleus can be found off ^{12}C cluster, but with a rather small probability. We note that an extra proton appears out of ^{12}C cluster a little bit more often than an extra neutron does mainly due to its Coulomb repulsion from the α-particles. It is demonstrated below that two maxima of curve *1* (and of the dashed line *3*) are a consequence of two spatial configurations distinctly present in ^{14}N nucleus.

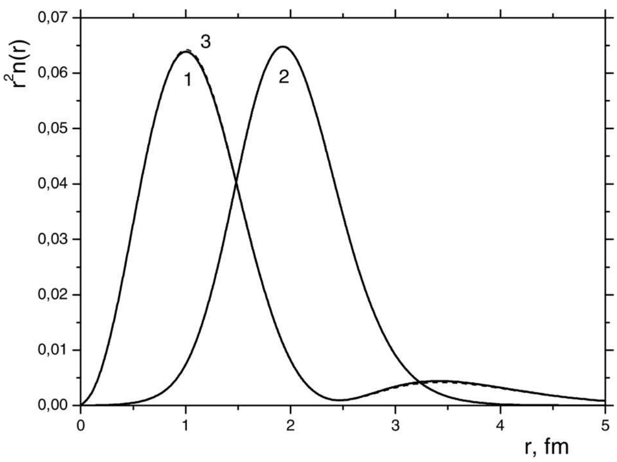

Fig. 1. Probability density distributions multiplied by r^2 obtained for an extra proton (solid curve *1*) and α-particles (solid curve *2*) in ^{14}N nucleus. Dashed line *3* depicts the same for an extra neutron

To find the charge r.m.s. radius of ^{14}N nucleus, we use the known Helm approximation [16, 17], which enables one, in a simple way, to take into account that particles are not "pointlike" ones. Within this approach, the charge density distribution for ^{14}N nucleus,

$$n_{\text{ch}}(r) = \frac{6}{7}\int n_\alpha\left(|\mathbf{r}-\mathbf{r}'|\right) n_{\text{ch},{}^4\text{He}}(r')\,d\mathbf{r}' + \\ +\frac{1}{7}\int n_p\left(|\mathbf{r}-\mathbf{r}'|\right) n_{\text{ch},p}(r')\,d\mathbf{r}', \tag{5}$$

is a sum of convolution products, first being the product of the density distribution n_α for the probability to find an α-particle inside the ^{14}N nucleus with the charge density distribution $n_{\text{ch},{}^4\text{He}}$ of an α-particle itself, while the second is the product of similar distributions for an extra proton. Coefficients before the integrals are proportional to the total charge of three α-clusters (6/7) and of an extra proton (1/7). The values of n_α and n_p are calculated within our five-particle model according to (4), while $n_{\text{ch},{}^4\text{He}}$ and $n_{\text{ch},p}$ follow from the experimental form factors [18] and [19], respectively. In relation (5), we neglect the small contribution of extra neutron. The normalization of the charge density distribution is $\int n_{\text{ch}}(r)\,d\mathbf{r} = 1$, i.e. one has to multiply it by Ze to obtain the necessary dimensional units.

In Fig. 2, the charge density distribution (5) of ^{14}N nucleus is shown (solid line *1*). In spite of the fact

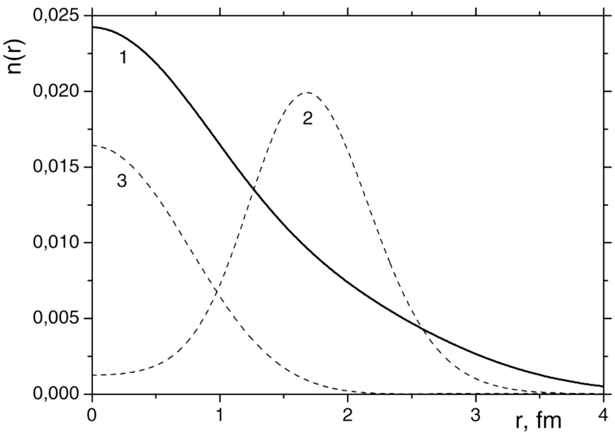

Fig. 2. Charge density distribution in ^{14}N nucleus (normalized as $\int n_{\mathrm{ch}}(r)\, d\mathbf{r} = 1$) – curve *1*. Dashed line *2* depicts the probability density distribution of "pointlike" α-particles in ^{14}N nucleus. Dashed line *3* is the density distribution $n_p(r)$ (multiplied by $\times 10^{-1}$) of a "pointlike" extra proton

that the density distribution of "pointlike" α-particles has a "dip" at short distances (see the dashed curve *2*), its integration with $n_{\mathrm{ch},^4\mathrm{He}}$ in (5) smoothes out this effect completely. The density distribution of an extra proton (dashed line *3* depicts $0.1 n_p$) makes a little influence on the total result due to a multiplier 1/7, but the proton also contributes at short distances and smoothes the tolal charge density distribution of the nucleus. A similar smooth behavior of the charge density distribution in the Helm approximation is obtained for ^{14}C nucleus with two extra neutrons, and, of course, for ^{14}O with two extra protons [6]. It is worth to note that the Helm approximation [16, 17] used in our model does not involve the exchange effects between identical nucleons present in the nuclei under consideration, and this approximation is a rather good one only if the clusters do not overlap. To improve the approximation and to obtain the almost accurate wave function of the nucleus (as noted in [1]), one has to multiply the obtained five-cluster wave function by the wave functions of α-particles (expressed in terms of the nucleon degrees of freedom) and then to carry out the antisymmetrization of the obtained fourteen-nucleon wave function over identical nucleons. This is beyond our study, and thus we omit a comparison of the results obtained in the Helm approximation for charge density distributions (and corresponding form factors) with experimental data.

Calculated r.m.s. relative distances and r.m.s. radii (fm) for ^{14}N nucleus

r_{pn}	$r_{p\alpha}$	$r_{n\alpha}$	$r_{\alpha\alpha}$	R_p	R_n	R_α	R_m	R_{ch}
2.237	2.692	2.683	3.559	1.598	1.585	2.064	2.556	2.558

The r.m.s. radius R_i of a probability density distribution $n_i(r)$ is known to be $R_i = \left(\int r^2 n_i(r)\, d\mathbf{r}\right)^{1/2}$. Having the wave function in the explicit form of a sum of Gaussian functions, we obtain the r.m.s. radii for ^{14}N nucleus within the five-particle model. In Table, the r.m.s. radii obtained for a "pointlike" extra proton R_p, extra neutron R_n, and α-particles R_α in ^{14}N nucleus are shown. We also give the calculated r.m.s. matter R_m and charge R_{ch} radii. For convenience, we give here also r.m.s. relative distances r_{ij} between particles (see the next section, where the definition of r_{ij} is given, and their relation to r.m.s. radii R_i is presented).

4. Pair Correlation Functions and Relative Distances

More information about the structure of a nucleus can be obtained from the analysis of the pair correlation functions. The pair correlation function $g_{ij}(r)$ for a pair of particles i and j can be defined as

$$g_{ij}(r) = \langle \Phi | \, \delta(\mathbf{r} - (\mathbf{r}_i - \mathbf{r}_j)) \, | \Phi \rangle, \tag{6}$$

and it is known to be the density of the probability to find the particles i and j at a definite distance r. These functions are normalized as $\int g_{ij}(r)\, d\mathbf{r} = 1$. The r.m.s. relative distances squared $\left\langle r_{ij}^2 \right\rangle$ are directly expressed through the pair correlation functions g_{ij}:

$$\left\langle r_{ij}^2 \right\rangle = \int r^2 g_{ij}(r)\, d\mathbf{r}. \tag{7}$$

The calculated r.m.s. relative distances $r_{ij} \equiv \left\langle r_{ij}^2 \right\rangle^{1/2}$ between particles in ^{14}N nucleus are given in Table. We note that the r.m.s. radii R_i are connected with the r.m.s. relative distances r_{jk}:

$$R_i^2 = \frac{1}{M^2} \left((M - m_i) \sum_{j \neq i} m_j r_{ij}^2 - \sum_{\substack{j < k \\ (j \neq i,\, k \neq i)}} m_j m_k r_{jk}^2 \right), \tag{8}$$

where M is the total mass of the system of particles. Thus, the r.m.s. radii R_i could be calculated not only directly through the density distributions, but also (equivalently) with the use of the pair correlation functions and relations (7) and (8). Note that the relative distances between particles are about (or even a little bit greater) than the sum of their own sizes. This fact substantiates, in part, the validity of our cluster model.

Since the average of a pairwise local potential $V_{ij}(r)$ is expressible directly through the pair correlation function $g_{ij}(r)$,

$$\langle \Phi | V_{ij} | \Phi \rangle = \int V_{ij}(r)\, g_{ij}(r)\, d\mathbf{r}, \tag{9}$$

the variational principle makes the profile of $g_{ij}(r)$ such that it has a maximum, where the potential is attractive, and a minimum in the area of repulsion (if the role of the kinetic energy is not crucial). The α-particles have about four times greater mass than extra nucleons, and, thus, their kinetic energy is essentially smaller than that of nucleons (see below). As a result, the pair correlation function $g_{\alpha\alpha}(r)$ profile is determined mainly by the potential $\hat{U}_{\alpha\alpha}$ and has a pronounced maximum (curve *1* in Fig. 3) near the minimum of the attraction potential. On the other hand, due to the presence of a local repulsion in the same potential near the origin, the profile of $g_{\alpha\alpha}(r)$ has a dip at short distances. Thus, the profile of $g_{\alpha\alpha}(r)$ shows that α-particles are mainly settled at a definite distance $r_{\alpha\alpha}$ one from another (see Table) being about the doubled radius of an α-particle, and they form a triangle of ^{12}C cluster. The same cluster is present in ^{14}C and ^{14}O nuclei, as seen from Fig. 4, where the pair correlation functions for ^{14}C nucleus are shown (we omit almost identical similar profiles for ^{14}O). But since the $\alpha\alpha$-potential used in the present work has somewhat greater radius than that accepted in [6], it is natural to obtain $r_{\alpha\alpha} \cong 3.6$ fm for ^{14}N nucleus instead of $r_{\alpha\alpha} \cong 3.2$ fm for ^{14}C and ^{14}O nuclei [6].

The deuteron cluster in ^{14}N formed by two extra nucleons has (on the average, from the qualitative point of view) almost the same form as a free deuteron, as seen from Fig. 3, where the $g_{pn}(r)$ function is shown for ^{14}N (solid curve *4*) to be compared with $g_{pn}(r) \equiv |\psi_{\mathrm{d}}(r)|^2$ for a free deuteron (dashed curve *5*). But, in ^{14}N, the deuteron cluster is more tightly bound than in a free state. That is why the asymptotics of the free deutron function $g_{pn}(r)$ goes above that of $g_{pn}(r)$ for ^{14}N nucleus, while below it at short distances (due to the normalization condition). The extra nucleon pair correlation function ($g_{nn}(r)$ for ^{14}C, as well as $g_{pp}(r)$ for ^{14}O), also has a dip at short distances (see Fig. 4, curve *2*) due to the presence of a short-range repulsion in our singlet nucleon-nucleon potential [3, 5, 6].

The functions $g_{p\alpha}(r)$ and $g_{n\alpha}(r)$ for ^{14}N nucleus have a small dip at short distances (see Fig. 3),

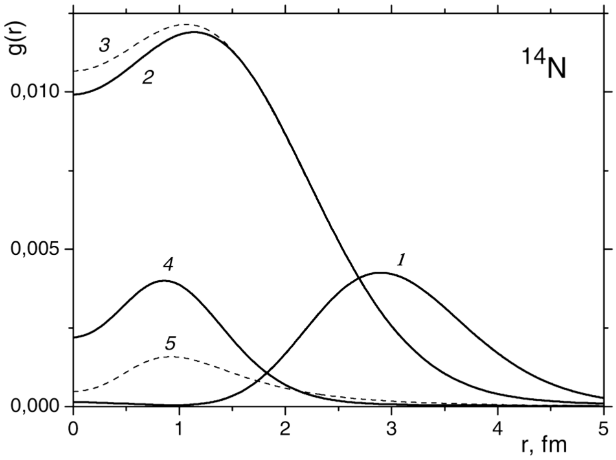

Fig. 3. Pair correlation functions for ^{14}N nucleus. Solid line *1* presents $g_{\alpha\alpha}(r)$, solid curve *2* depicts $g_{p\alpha}(r)$, and dashed line *3* corresponds to $g_{n\alpha}(r)$. Curve *4* is the pair correlation function (multiplied by 0.1) for extra nucleons, $0.1 g_{pn}(r)$, and dashed line *5* is the wave function squared of the deuteron (multiplied by 0.1)

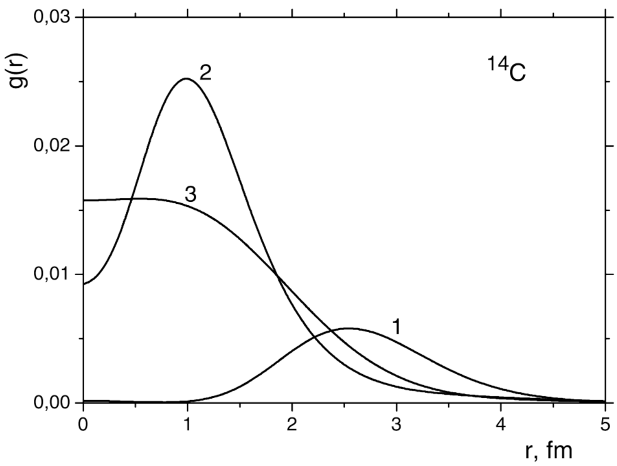

Fig. 4. Pair correlation functions for ^{14}C nucleus: $g_{\alpha\alpha}(r)$ – curve *1*, $g_{nn}(r)$ – curve *2*, and $g_{n\alpha}(r)$ – curve *3*

while the corresponding functions $g_{n\alpha}(r)$ for ^{14}C and $g_{p\alpha}(r)$ for ^{14}O have no pronounced dips at all (see Fig. 4 for ^{14}C). Almost the same profile is revealed by $g_{p\alpha}(r)$ for ^{14}O, which is not shown. The fact that the above-mentioned correlation functions do not vanish at short distances can be explained by the absence of a short-range local repulsion in our model of generalized potential between a nucleon and an α-particle. This potential contains the local pure attraction plus the nonlocal (separable) repulsion with greater radius [6].

5. Two Configurations in ^{14}N, ^{14}C, and ^{14}O Nuclei

To make the structure of the ground state of ^{14}N nucleus (as well as of ^{14}C and ^{14}O nuclei) more clear, let us consider the quantity $P(r,\rho,\theta)$ proportional to the density of the probability to find extra nucleons at a definite relative distance r and to find their center of mass at a distance ρ from the center of mass of ^{12}C cluster:

$$P(r,\rho,\theta) = \\ = r^2\rho^2 \langle\Phi|\,\delta(\mathbf{r}-\mathbf{r}_{NN})\,\delta\left(\boldsymbol{\rho}-\boldsymbol{\rho}_{(NN),(3\alpha)}\right)|\Phi\rangle, \qquad (10)$$

where θ is the angle between the vectors $\mathbf{r}$ and $\boldsymbol{\rho}$. It is assumed that $\theta = 0°$ corresponds to a spatial configuration, where the extra proton, extra neutron, and center of mass of ^{12}C cluster are at the same line, the proton being further from ^{12}C than the neutron. The angle $\theta = 180°$ corresponds to almost the same configuration, but with an extra neutron located further from the center of mass of ^{12}C cluster. If one considers ^{14}C and ^{14}O nuclei, the configurations with $\theta = 0°$ and $\theta = 180°$ are identical due to identical extra nucleons. Although these two angles are not identical for ^{14}N nucleus, the configurations with a definite θ and $180° - \theta$ are very similar (approximately identical), since the role of the Coulomb interaction is not decisive. That is why we do not demonstrate the profiles of $P(r,\rho,\theta)$ for $\theta > 90°$ in the figures.

The quantity $P(r,\rho,\theta)$ for ^{14}N nucleus is depicted in Fig. 5 for $\theta = 0°$, $\theta = 30°$, $\theta = 45°$, and $\theta = 90°$ as a function of r and ρ. Two peaks on the $P(r,\rho,\theta)$ surface are observed at $\theta = 0°$ (as well as for $\theta = 180°$, which is not shown), and only one peak at $\theta = 90°$. The rest angles give intermediate results (see Fig. 5 for $\theta = 30°$ and $\theta = 45°$). If it were not the multiplier $r^2\rho^2$ in (10), the main peak present at all the angles θ would be settled just at $\rho = 0$, i.e. the center of mass of ^{12}C cluster and that of the deuteron one would coincide. The comparatively smaller (than a free deuteron, see Fig. 3) deuteron cluster moves mainly inside ^{12}C cluster. The second peak reveals itself mainly at $\theta = 0°$ and corresponds to a configuration, where an extra neutron is located inside ^{12}C cluster, while an extra proton is comparatively far from the center of the nucleus (it is out of ^{12}C cluster). At $\theta = 180°$, almost the same configuration is observed (not shown in the figure). But, in this case, an extra proton is inside ^{12}C cluster. Just these configurations make a contribution to the second maximum of the extra nucleon probability density distribution (see Fig. 1). In this configuration, the center of mass of the subsystem of extra nucleons does not coincide with the center of mass of ^{12}C cluster. The almost same (from the qualitative point of view) two configurations are observed in the ground state of ^{14}C nucleus (see Fig. 6) or ^{14}O one (not shown for brevity, since the corresponding pictures almost coincide with those depicted in Fig. 6). Note that a configuration with one nucleon out of ^{12}C cluster is more pronounced in the case of mirror nuclei ^{14}C and ^{14}O as compared to ^{14}N nucleus, because the interaction potential in the singlet state between extra nucleons is less strong than the interaction potential in the triplet state, which compels a proton and a neutron to be coupled inside a five-particle system with greater probability. We also note that a small difference in $\alpha\alpha$-interactions used in calculations of the ^{14}N and ^{14}C nuclei ground states makes almost no influence on the effect of two configurations. We carried out a number of test calculations with $\alpha\alpha$-potentials, which result in different values of the binding energy of ^{12}C nucleus. The results for the ground states of ^{14}N and ^{14}C nuclei are similar to those shown in Figs. 5 and 6.

A similar situation with two configurations in the ground state is found for ^{6}He, ^{6}Li [1–3, 12] or ^{10}Be, ^{10}C [4, 5] nuclei, where the center of mass of the dinucleon subsystem coincides (one configuration) or does not coincide (another configuration) with the center of mass of the subsystem of α-particles.

6. Momentum Distributions

To complete the study of the structure functions of ^{14}N nucleus, we present the momentum distributions

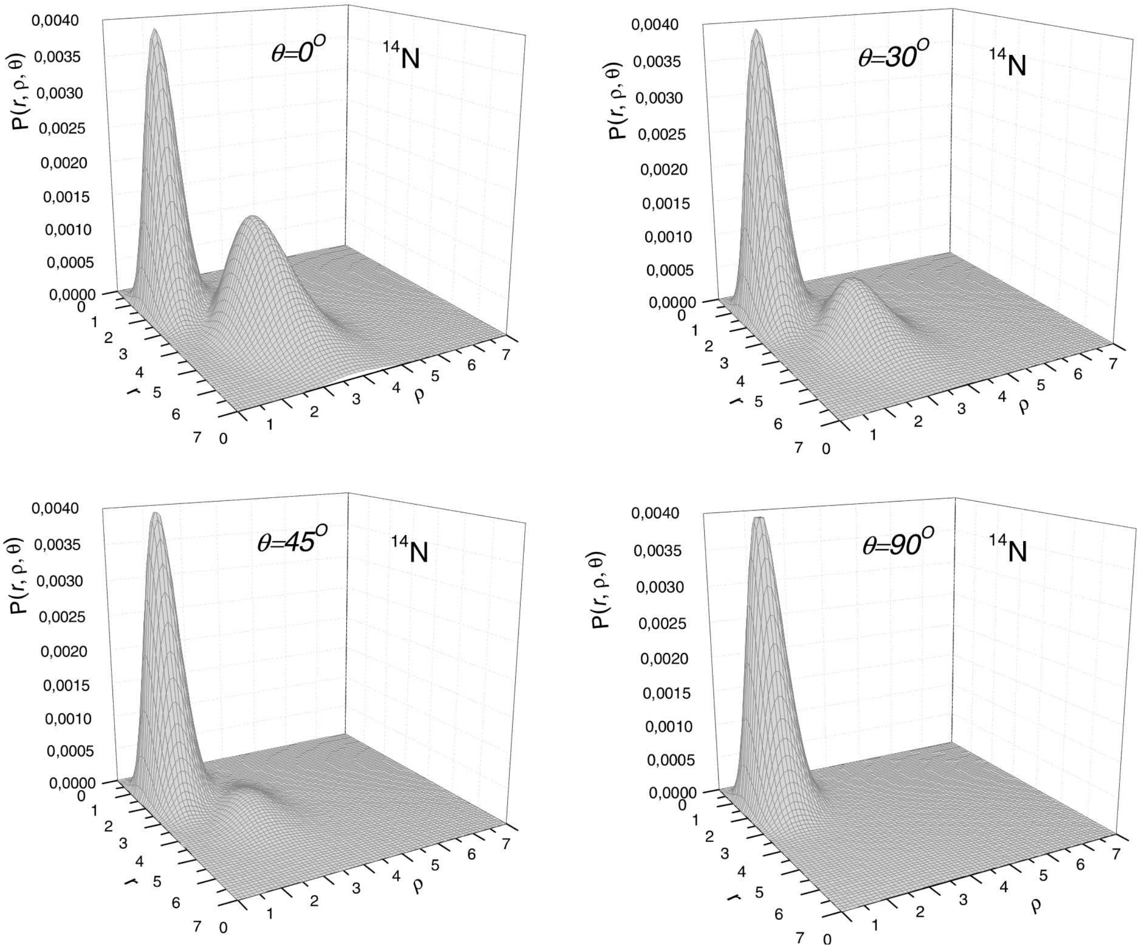

Fig. 5. Two configurations in the ground state of ^{14}N nucleus manifesting themselves in the $P\left(r,\rho,\theta\right)$ function at different angles θ

of α-particles and extra nucleons in this system within the five-particle model. The momentum distribution $n_i\left(k\right)$ of the i-th particle is known to be the density of the probability to find this particle with a definite momentum k,

$$n_i\left(k\right)=\left\langle\tilde{\Phi}\right|\delta\left(\mathbf{k}-\left(\mathbf{k}_i-\mathbf{K}_{c.m.}\right)\right)\left|\tilde{\Phi}\right\rangle, \tag{11}$$

where $\tilde{\Phi}$ is the wave function of the system in the momentum representation. The normalization of the momentum distribution is $\int n_i\left(k\right)d\mathbf{k}=1$. The momentum distribution $n_i\left(k\right)$ enables one, in particular, to calculate the average kinetic energy of the i-th particle:

$$\left\langle E_{i,\mathrm{kin}}\right\rangle=\int\frac{k^2}{2m_i}n_i\left(k\right)d\mathbf{k}. \tag{12}$$

Mainly due to the mass ratio between a nucleon and an α-particle, the extra nucleons move much more rapidly than the α-particles do. In particular, the average kinetic energy of an extra proton in ^{14}N nucleus is about 33.52 MeV, that of an extra neutron equals about 33.53 MeV, while each of the more slowly moving α-particles has the kinetic energy of about 5.79 MeV. Similar values are typical of ^{14}C and ^{14}O nuclei. In particular, the calculated kinetic energy of each of the extra neutrons in ^{14}C nucleus is about 32.66 MeV, while the same value for an α-particle amounts about 6.83 MeV. For ^{14}O nucleus, we have 31.77 MeV for an extra proton and 6.62 MeV for an α-particle. The corresponding ratio of velocities is about 4.8 for ^{14}N nucleus and about 4.4 for ^{14}C and ^{14}O nuclei. This means that the extra nucleons of

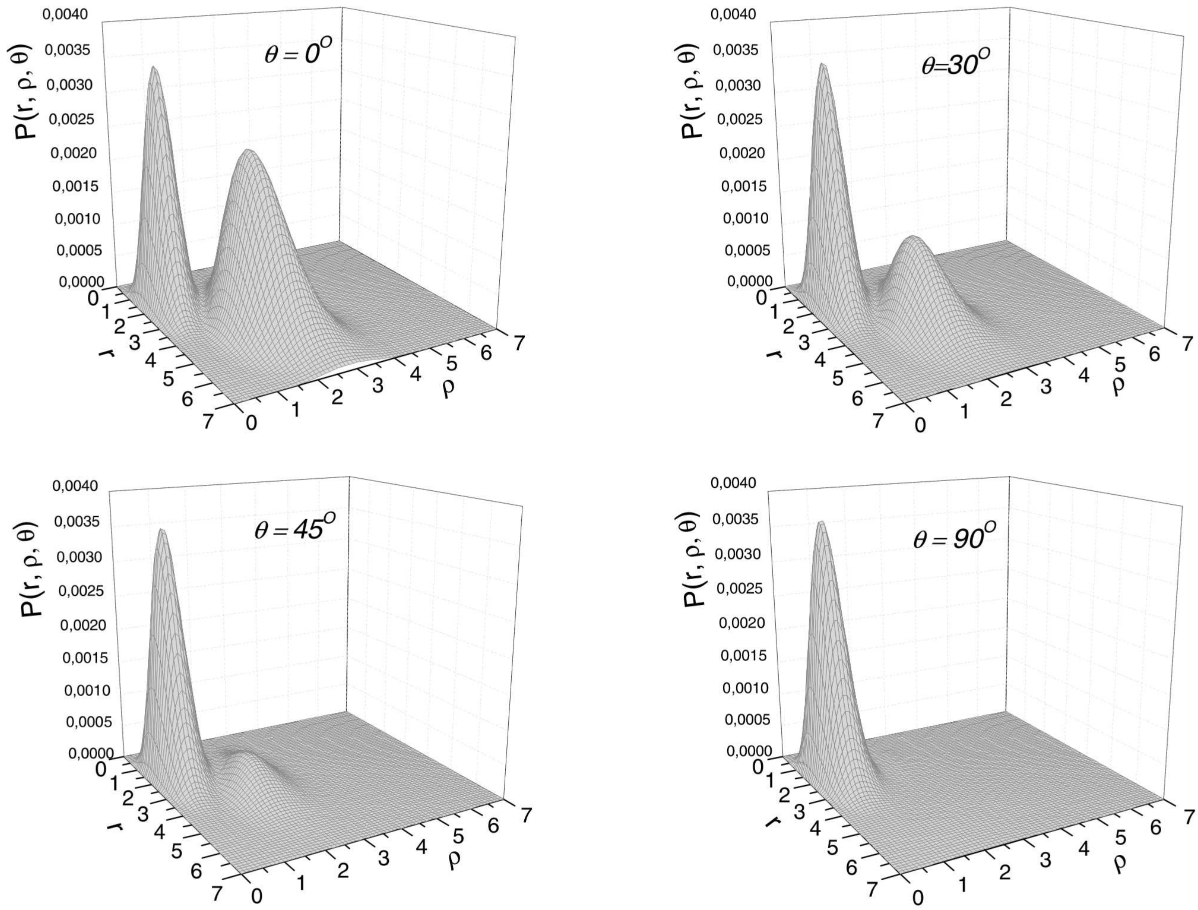

Fig. 6. Two configurations in the ground state of ^{14}C nucleus

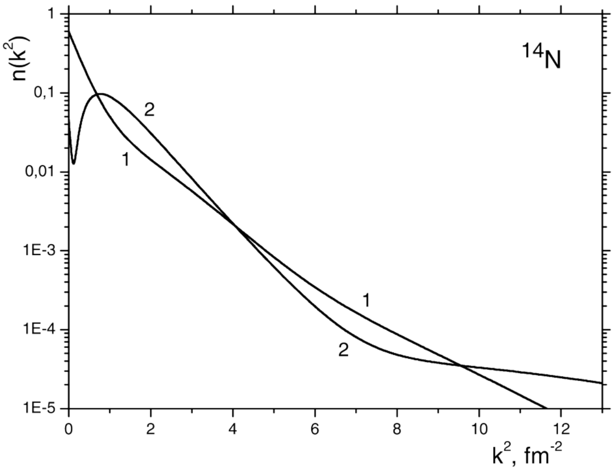

Fig. 7. Momentum distributions of an α-particle (curve *1*) and an extra proton (curve *2*) in ^{14}N nucleus

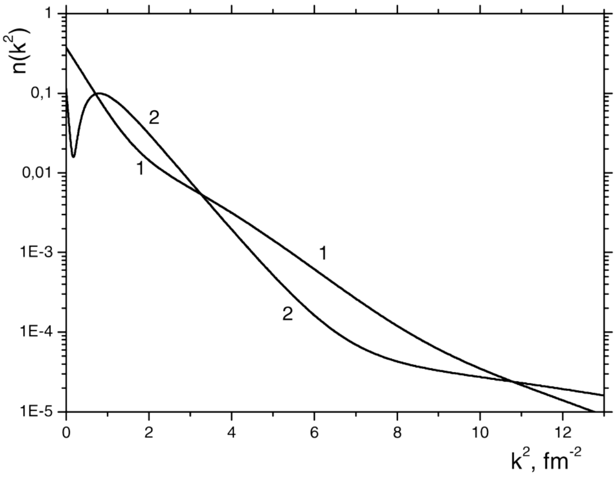

Fig. 8. Momentum distributions of an α-particle (curve *1*) and an extra neutron (curve *2*) in ^{14}C nucleus

the nuclei under consideration move essentially faster than the heavier α-particles do.

The momentum distributions of α-particles, as well as those of extra nucleons, are very similar for all the considered nuclei. Especially, they are close for ^{14}C and ^{14}O nuclei. That is why we present the profiles of the momentum distributions only for ^{14}N (Fig. 7) and ^{14}C (Fig. 8). In Fig. 7, curve *1* corresponds to the momentum distribution $n_\alpha(k)$ of an α-particle, and curve *2* depicts $n_p(k)$ of an extra proton. The momentum distribution of an extra neutron $n_n(k)$ is not shown, because the corresponding curve almost coincides with curve *2*. Very similar (from the qualitative point of view) profiles of the momentum distributions are obtained for ^{14}C and ^{14}O nuclei (see Fig. 8 for ^{14}C; almost the same profiles could be depicted for ^{14}O nucleus).

The momentum distribution of α-particles $n_\alpha(k)$ is seen to be a monotonically decreasing function, while $n_p(k)$ and $n_n(k)$ have two maxima: at the zero momentum and at $k^2 \simeq 1$ fm^{-2}. These two maxima correspond to two above-mentioned configurations in the ground state of the nucleus. In a configuration, where an extra nucleon is comparatively far from the center of the nucleus, it moves comparatively slowly and makes a contribution to the peak at very small k^2. If it is inside ^{12}C cluster (and this may occur in both spatial configurations), its momentum is somewhat greater, and such momenta make their contribution to the second maximum at $k^2 \simeq 1$ fm^{-2}. At the same time, the heavier α-particles inside ^{12}C cluster almost do not feel peculiarities of the motion of extra nucleons. Thus, the influence of two different spatial configurations of extra nucleons on the momentum distribution of α-particles is small due to both the mass ratio and the comparatively large binding energy of ^{12}C cluster.

7. Conclusions

To sum up, we note that the spatial structure of ^{14}N nucleus studied within the five-particle model is very similar to the structure of the mirror nuclei ^{14}C and ^{14}O. Two configurations in the ground-state wave functions of these nuclei are revealed, where ^{12}C cluster and the dinucleon subsystem have the same centers of mass (first configuration, with a dinucleon inside ^{12}C cluster) or the shifted centers of mass (second configuration, with one nucleon outside of ^{12}C cluster). These configurations manifest themselves, in particular, in the density and momentum distributions. A similar situation with two configurations in the ground state of the system is inherent in some other light nuclei [1–5] with two extra nucleons.

This work was supported in part by the Program of Fundamental Research of the Division of Physics and Astronomy of the NAS of Ukraine (project No. 0117U000240).

1. V.I. Kukulin, V.N. Pomerantsev, Kh.D. Razikov, V.T. Voronchev, G.G. Ryzhikh. Detailed study of the cluster structure of light nuclei in a three-body model (IV). Large space calculation for A = 6 nuclei with realistic nuclear forces. *Nucl. Phys. A* **586**, 151 (1995).
2. M.V. Zhukov, B.V. Danilin, D.V. Fedorov, J.M. Bang, I.J. Thompson, J.S. Vaagen. Bound state properties of Borromean halo nuclei: ^{6}He and ^{11}Li. *Phys. Reports* **231**, 151 (1993).
3. B.E. Grinyuk, I.V. Simenog. Structure of the ^{6}He nucleus in the three-particle model. *Physics of Atomic Nuclei* **72**, 6 (2009).
4. Y. Ogawa, K. Arai, Y. Suzuki, K. Varga. Microscopic four-cluster description of ^{10}Be and ^{10}C with the stochastic variational method. *Nucl. Phys. A* **673**, 122 (2000).
5. B.E. Grinyuk, I.V. Simenog. Structural properties of the ^{10}Be and ^{10}C four-cluster nuclei. *Physics of Atomic Nuclei* **77**, 415 (2014).
6. B.E. Grinyuk, D.V. Piatnytskyi. Structure of ^{14}C and ^{14}O nuclei calculated in the variational approach. *Ukr. J. Phys.* **61**, 674 (2016).
7. A.V. Nesterov, F. Arickx, J. Broeckhove, V.S. Vasilevsky. Three-cluster description of properties of light neutron- and proton-rich nuclei in the framework of the algebraic version of the resonating group method. *Phys. Part. Nucl.* **41**, 716 (2010).
8. V.I. Kukulin, V.M. Krasnopol'sky. A stochastic variational method for few-body systems. *J. Phys. G: Nucl. Phys.* **3**, 795 (1977).
9. Y. Suzuki, K. Varga. *Stochastic Variational Approach to Quantum-Mechanical Few-Body Problems* (Springer, 1998) [ISBN: 978-3-540-65152-9].
10. B.E. Grinyuk, I.V. Simenog. Three-particle structure of the halo nucleus ^{6}Li. *Nuclear Physics and Atomic Energy* **10**, 9 (2009).
11. B.E. Grinyuk, I.V. Simenog. Structure peculiarities of three- and four-cluster nuclei ^{6}He, ^{6}Li, and ^{10}Be, ^{10}C. *Nuclear Physics and Atomic Energy* **12**, 7 (2011).
12. B.E. Grinyuk, I.V. Simenog. Asymptotic features of density distributions and form factors for ^{6}Li and ^{6}He nuclei in the three-particle model. *Ukr. J. Phys.* **55**, 369 (2010).
13. V.G. Neudatchin, V.I. Kukulin, V.L. Korotkikh, V.P. Korennoy. A microscopically substantiated local optical potential for α-α-scattering. *Phys. Lett. B* **34**, 581 (1971).
14. V.I. Kukulin, V.G. Neudatchin, Yu.F. Smirnov. Composite particle interaction relevant to the Pauli principle. *Fiz.*

Élem. Chastits At. Yadra **10**, 1236 (1979) (*Sov. J. Part. Nucl.* **10**, 492 (1979)).

15. I. Angeli, K.P. Marinova. Table of experimental nuclear ground state charge radii: An update. *Atomic Data and Nuclear Data Tables* **99**, 69 (2013).
16. R.H. Helm. Inelastic and elastic scattering of 187-Mev electrons from selected even-even nuclei. *Phys. Rev.* **104**, 1466 (1956).
17. A.I. Akhiezer, V.B. Berestetskii. *Quantum Electrodynamics* (Interscience, 1965) [ISBN: 0470018488].
18. R.F. Frosch, J.S. McCarthy, R.E. Rand, M.R. Yearian. Structure of the He^4 nucleus from elastic electron scattering. *Phys. Rev.* **160**, 874 (1967).
19. P.E. Bosted *et al.* Measurements of the electric and magnetic form factors of the proton from $\bar{Q}^2 = 1.75$ to 8.83 $(\mathrm{GeV}/c)^2$. *Phys. Rev. Lett.* **68**, 3841 (1992).

Received 30.08.17

Б.Є. Гринюк, Д.В. П'ятницький

СТРУКТУРА ЯДРА ^{14}N У П'ЯТИКЛАСТЕРНІЙ МОДЕЛІ

Р е з ю м е

Досліджено просторову структуру ядра ^{14}N в рамках п'ятичастинкової моделі (три α-частинки і два нуклони). Розраховано енергію і хвильову функцію основного стану цієї п'ятичастинкової системи на основі варіаційного підходу з використанням гаусоїдних базисів. Виявлено дві просторові конфігурації хвильової функції основного стану. Проаналізовано розподіли густини, парні кореляційні функції і імпульсні розподіли частинок в ядрі ^{14}N та порівняно із відповідними розподілами для дзеркальних ядер ^{14}C і ^{14}O.